Structural characterisation of a VMgO catalyst used in the oxidative dehydrogenation of propane

Andrew Burrows [a,*], Christopher J. Kiely [a], Jens Perregaard [b], Poul E. Højlund-Nielsen [b], Gert Vorbeck [b], Jose J. Calvino [c] and Carlos López-Cartes [c]

[a] *Department of Engineering, Materials Science and Engineering, The University of Liverpool, Merseyside L69 3BX, UK*
E-mail: ab0895@liv.ac.uk
[b] *Haldor Topsøe A/S, Nymøllevej 55, DK-2800 Lyngby, Denmark*
[c] *Departamento de Ciencia de los Materiales e Ingeniería Metalúrgica y Química Inorgánica, Universidad de Cádiz, Apdo 40, Puerto Real, 11510 Cádiz, Spain*

Received 22 October 1998; accepted 3 December 1998

A VMgO catalyst (containing 14 wt% vanadium) that is used in the oxidative dehydrogenation of propane (ODHP) reaction has been examined in detail by *in situ* EXAFS, *in situ* XRD and HREM. These characterisation techniques have revealed that, as prepared, the catalyst is in effect a three-component system comprising discrete magnesium orthovanadate ($Mg_3V_2O_8$) particles, magnesium oxide and a disordered vanadium-containing overlayer supported on the MgO. When the catalyst is exposed to typical ODHP reaction conditions at 500 °C the *in situ* EXAFS indicates a change in vanadium oxidation state from 5+ to 3+. Under the same conditions, *in situ* XRD suggests that $Mg_3V_2O_8$ transforms to a cubic spinel type structure with a lattice parameter of 8.42 Å. These changes are reversible on exposure to air at 500 °C. HREM shows that the overlayer on MgO changes from a disordered state to a weakly ordered structure after exposure to normal reaction conditions whilst pure propane (strongly reducing conditions) induces pronounced structural ordering of the overlayer. Image simulations have led us to the conclusion that the ordered layer comprises a cubic spinel (MgV_2O_4) phase in parallel epitaxy with the MgO support. The surface regions of the bulk $Mg_3V_2O_8$ particles are also found to undergo structural modification under typical reaction conditions decomposing to a mixture of MgO crystallites and MgV_2O_4; strong reduction causes a complete conversion to MgV_2O_4.

Keywords: VMgO catalyst, magnesium oxide, magnesium orthovanadate, oxidative dehydrogenation of propane, structural characterisation, *in situ* characterisation, high-resolution electron microscopy, image simulations

1. Introduction

The oxidative dehydrogenation of propane (ODHP) is one of the few examples of the direct conversion of an alkane to more useful products. In this case, the reaction proceeds in the presence of molecular oxygen to give the alkene, propene (equation (1)), although undesired oxygenated by-products, principally CO_2, which are more thermodynamically favourable, can also be produced (equation (2)) [1]:

$$C_3H_8 + (1/2)O_2 \rightarrow C_3H_6 + H_2O \quad (1)$$

$$C_3H_8 + 5O_2 \rightarrow 3CO_2 + 4H_2O \quad (2)$$

The vanadium magnesium oxide (VMgO) catalyst system has previously been reported to be effective in the ODHP reaction showing a high selectivity for propene [2–4], as well as promoted VMgO catalyst systems [5,6]. More recently [7,8], low vanadium contents and high calcination temperatures have been shown to give good catalytic performance. The highest propene yields were obtained when the vanadium content was approximately 14 wt% after calcination at a temperature of 800 °C. No structure sensitivity was reported for selectivity to propene, whilst intrinsic activity was found to depend very much on the structure of the catalyst.

As noted by Oganowski et al. [9], there is some controversy concerning the active phase for this type of catalyst, most literature proposals favouring a bulk VMgO phase (either $Mg_2V_2O_7$ or $Mg_3V_2O_8$). However, more recently [10], it has been suggested that monomeric and polymeric vanadia species supported on MgO (that undergo reversible disorder/order restructuring under redox cycles) are the source of catalytic activity. The work presented in this paper complements and extends the microstructural characterisation reported by Pantazidis et al. [10] by studying in detail the transformation of the V-containing layer in a 14 wt% vanadium VMgO catalyst under different reaction atmospheres. *In situ* XRD and *in situ* EXAFS studies, high-resolution electron microscopy (HREM) and image simulation have been used to determine the nature of the structural transformations occurring in the supported overlayer and the bulk $Mg_3V_2O_8$ phase.

2. Experimental

2.1. Catalyst preparation

Using a potassium hydroxide solution, $Mg(OH)_2$ was precipitated from a solution containing 110 g of $Mg(NO_3)_2$·

* To whom correspondence should be addressed.

$6H_2O$. After washing the precipitate and drying overnight at 120 °C, the solid was again washed and finally dried for 6 h at 120 °C in an N_2 atmosphere. The $Mg(OH)_2$ was then added to a hot (87 °C) solution of ammonium hydroxide, NH_4OH, containing 7.45 g of ammonium metavanadate, NH_4VO_3, with continuous stirring. The resulting suspension was evaporated to dryness followed by further drying at 120 °C and calcination at 800 °C for 6 h. Chemical analysis showed the vanadium content to be approximately 13.5 wt% corresponding to a total metal content (V/(V + Mg)) of about 0.127 – this material is referred to as the 14V/VMgO catalyst. Under normal working conditions, i.e., 1% C_3H_8/0.1% O_2/He (balance), this catalyst gives a propane conversion of approximately 11% and has a propene selectivity of around 70%.

2.2. Microstructural characterisation

2.2.1. Electron microscopy

Transmission electron microscopy (TEM) and HREM were carried out in a Jeol 2000EX microscope operating at 200 kV. Samples for TEM examination were prepared by gently grinding the powder in ethanol and dispersing the slurry onto a 3.05 mm holey-carbon-coated copper grid. EDX analyses on the 14V/VMgO catalyst were performed in a Jeol 2000FXII microscope operating at 200 kV.

2.2.2. Image simulation

All the supercells employed as input models for the image simulations have been modelled using the RHODIUS programme [11]. HREM image calculation was performed using the multislice routines of the EMS package [12] running on an Indy 4400SC Silicon Graphics workstation. A conventional CCD camera with a resolution of 512×512 pixels has been used to digitise the micrographs. Image processing of these digital images has been performed using the PC version of SEMPER 6+ software by Synoptics.

2.2.3. X-ray diffraction

Ex situ X-ray powder diffraction patterns were recorded in air by slow scanning on a Philips vertical goniometer equipped with a θ-compensating divergence slit and a diffracted beam graphite monochromator utilising Cu K-$L_{2,3}$ radiation. To determine the nature of any phase transformations that take place during reaction, *in situ* XRD experiments were carried using a custom designed cell built to Debye–Scherrer geometry. The XRD patterns were collected continuously (and integrated every 30 min) by a one-dimensional position sensitive detector (INEL (CPS 120)) over an angular range of 120° with an angular accuracy of 0.03°. The 14V/VMgO catalyst was subjected to typical ODHP reaction conditions and a reoxidation step in air at 500 °C.

2.2.4. EXAFS

In situ EXAFS experiments were carried out at the EXAFS II beam line of HASYLAB at DESY, Hamburg, Germany, which is equipped with a Si(111) double-crystal monochromator and Ni mirrors. Samples were studied in air and typical reaction conditions at a temperature of 500 °C to monitor any changes in the oxidation state of the vanadium in the catalyst.

3. Results

3.1. EXAFS

The X-ray absorption spectrum obtained in air at room temperature from the unused 14V/VMgO catalyst at the vanadium K-edge is shown in figure 1(a). A reference spectrum from V_2O_5 is also displayed (dashed line). A comparison between the size of the pre-peaks and the position of the edges indicates that the vanadium in the catalyst is in a 5+ oxidation state. However, after heating up to 500 °C

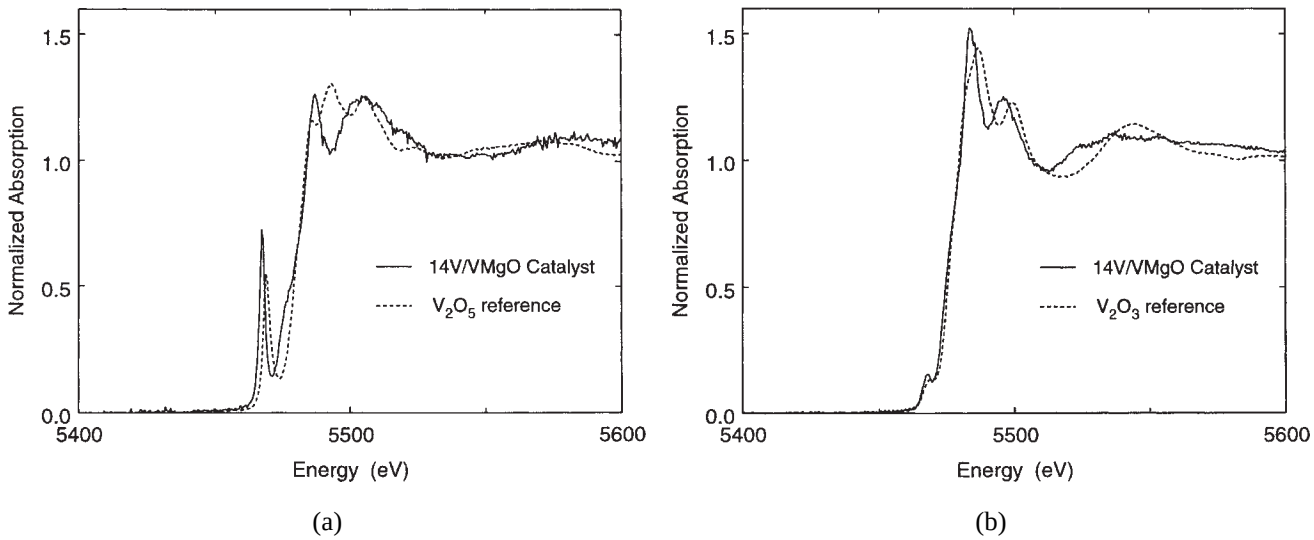

Figure 1. EXAFS spectra obtained at the vanadium K-edge from (a) the unused 14V/VMgO catalyst at room temperature compared to a V_2O_5 reference sample and (b) *in situ* at 500 °C under typical ODHP reaction conditions compared to a V_2O_3 reference sample.

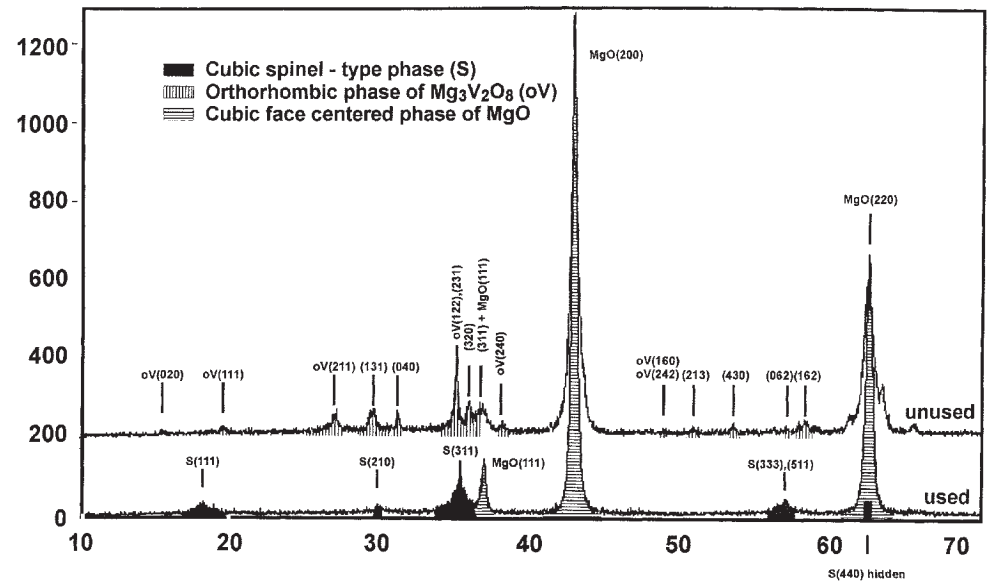

(a)

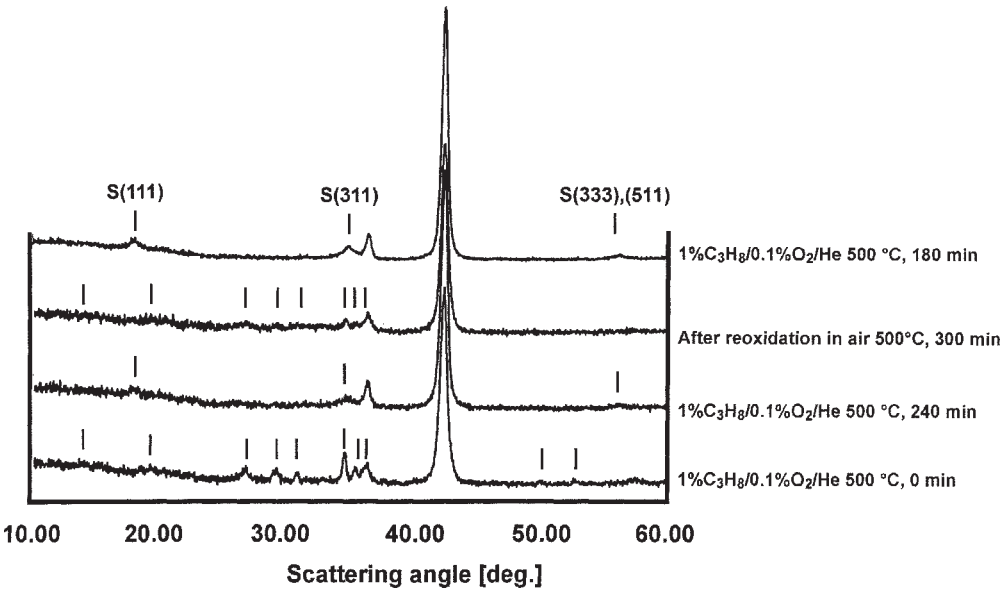

(b)

Figure 2. (a) Comparison of XRD patterns obtained from the 14V/VMgO catalyst in the unused and used (*in situ*) states. (b) *In situ* XRD patterns recorded under ODHP conditions at 500 °C for 0 and 240 min, reoxidised in air for 300 min and, finally, under ODHP conditions for a further 180 min.

in an atmosphere of 1% C_3H_8/0.1% O_2/He (balance), there is a significant change in the spectrum which is shown in figure 1(b). The full drawn trace in the figure is compared with a standard V_2O_3 reference spectrum (dashed line) and, again, by comparing the pre-peak and position of the edge, it is evident that the oxidation state of the catalyst is now closer to 3+. If the atmosphere is subsequently switched to air at 500 °C, the vanadium reverts back to the 5+ oxidation state.

3.2. X-ray diffraction

Figure 2(a) shows two superimposed XRD patterns of the 14V/VMgO catalyst; in the unused state, top, and after the catalyst had been subjected to ten catalytic ODHP cycles (used), bottom. Each cycle consisted of four steps:

(i) reaction of the propane/nitrogen mixture with the catalyst;

(ii) purge;

(iii) reoxidation of the catalyst (exposed to air);

(iv) purge before starting next cycle.

Based on a constant molar ratio between the alkane and vanadium, the tests were performed at 500 °C at atmospheric pressure and with a GHSV of 1000 Nl/h kg_{cat}. As expected, the pattern of the unused sample consists of a number of reflections that can be assigned to MgO

and orthorhombic magnesium orthovanadate (as a minor phase). However, in the "used" pattern, the reflections due to $Mg_3V_2O_8$ have disappeared and there is the appearance of other, rather weak, reflections that have been found from structural analysis to be consistent with a cubic spinel type phase, MgV_2O_4, with a lattice parameter of 8.42 Å.

The reversibility of the structural changes taking place in the catalyst inferred from the *in situ* EXAFS results was reproduced in the *in situ* XRD experiments. A few patterns from the numerous XRD patterns recorded at different temperatures under different gaseous atmospheres and run times is shown in figure 2(b). The first pattern was recorded just after reaching 500 °C and immediately switching to a reducing atmosphere containing 1% propane. It shows reflections that can only be assigned to MgO and $Mg_3V_2O_8$. After exposure to this atmosphere for 4 h, all of the reflections arising from the orthovanadate disappear and the cubic spinel phase is formed as indicated by the appearance of the 111, 311, 333 and 511 reflections. After reoxidation in air at 500 °C for 5 h, some of the reflections from $Mg_3V_2O_8$ reappear. Although the observed phase transformation is reversible, the back transformation from a cubic spinel structure to the magnesium orthovanadate appears to result in $Mg_3V_2O_8$ with an inferior degree of crystallinity compared to the as-prepared sample (figure 2(a)). Subsequent treatment under ODHP conditions for 3 h gives rise to reflections typical of the cubic spinel structure.

3.3. Electron microscopy

Both MgO and $Mg_3V_2O_8$ were observed in the TEM in the unused 14V/VMgO catalyst. MgO was found to be the dominant morphology in the form of platelets (100–200 nm in size) terminated by {111} planes. This unusual polar termination has been shown in previous publications [10,13] to arise due to a topotactic transformation from the parent brucite, $Mg(OH)_2$, phase. The magnesium orthovanadate particles that were occasionally observed were found to be approximately 80–150 nm in size. HREM and EDX analysis of the 14V/VMgO catalyst revealed the presence of a (disordered) V-containing layer on the MgO, an example of which is shown in figure 3(a). After the catalyst has been subjected to a flowing propane/helium/oxygen atmosphere for 4 h at 500 °C, the disordered overlayer develops small patches of a weakly ordered structure, as shown in figure 3(b). Unfortunately, it is difficult to extract any meaningful conclusions from measurement of the unidirectional lattice fringe spacings (which vary between 4.5 and 5.5 Å) running parallel to the MgO {111} planes although it is suspected the overlayer is epitaxial with the MgO support. Since the effect of typical ODHP reaction conditions is to reduce VMgO, the 14V/VMgO catalyst was subjected to a more aggressive reducing environment by using pure propane at 500 °C for 4 h and subsequently examined by TEM. Figure 3(c) is an HREM micrograph of an MgO platelet viewed edge-on after such a treatment in which a set of MgO {111} planes, running

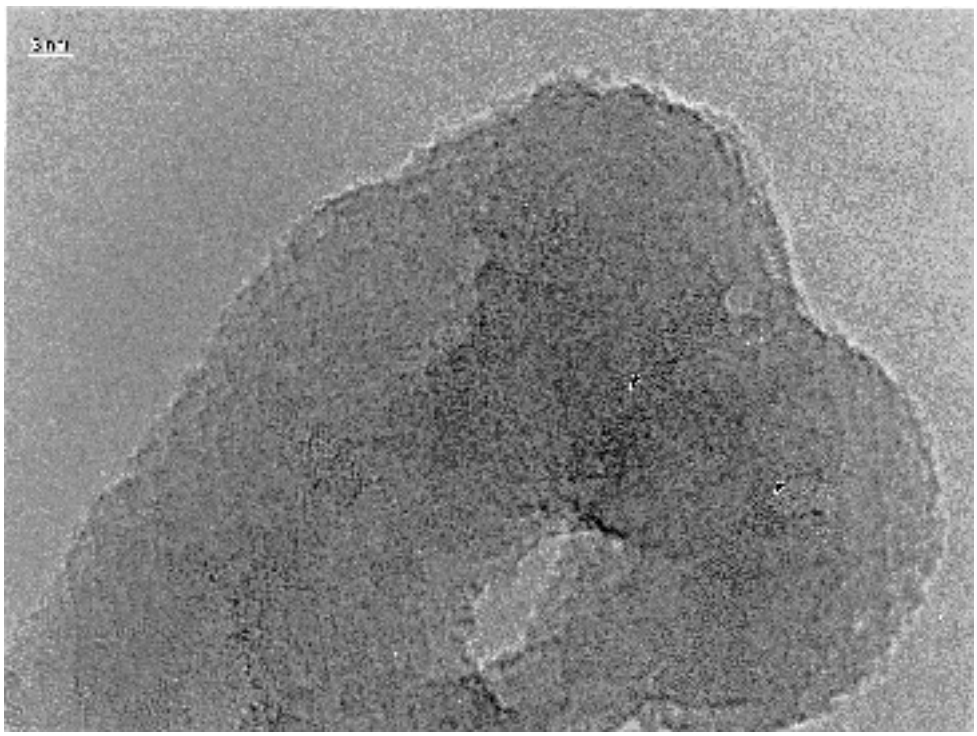

(a)

Figure 3. (a) The disordered V-containing overlayer supported on MgO as observed in the unused catalyst. (b) The weakly ordered structure of the overlayer after exposing the catalyst to typical ODHP reaction conditions. (c) The highly ordered overlayer structure after the catalyst has been exposed to pure propane: (A) in profile, (B) an extended plan-view patch; the arrows indicate two very thin regions.

parallel with the platelet surface, is resolved. The overlayer now exhibits extended patches of a highly ordered structure. Subsequent treatment in air at 500 °C for 5 h causes the overlayer to revert to a disordered state like that shown in figure 3(a).

In the region labelled "A" in figure 3(c), the overlayer is seen in profile on the MgO surface and appears to be approximately 10–15 Å thick. However, the overlayer is most often observed in plan-view as exemplified by the extended region labelled "B". The variations in contrast are indicative of significant differences in thickness across the layer; several very thin regions are just about visible and two have been arrowed on the figure. Parallel to the MgO (111) surface planes, the lattice fringe periodicity of the overlayer is 4.95 Å. A second set of overlayer fringes intersects these at approximately 68° with a spacing 4.69 Å. These periodicities and interplanar angles are not consistent with the bulk VMgO phases $Mg_2V_2O_7$ or MgV_2O_6. Neither do they correspond to the vanadium oxides V_2O_3, V_2O_4 or V_2O_5. There are two viable options for

(b)

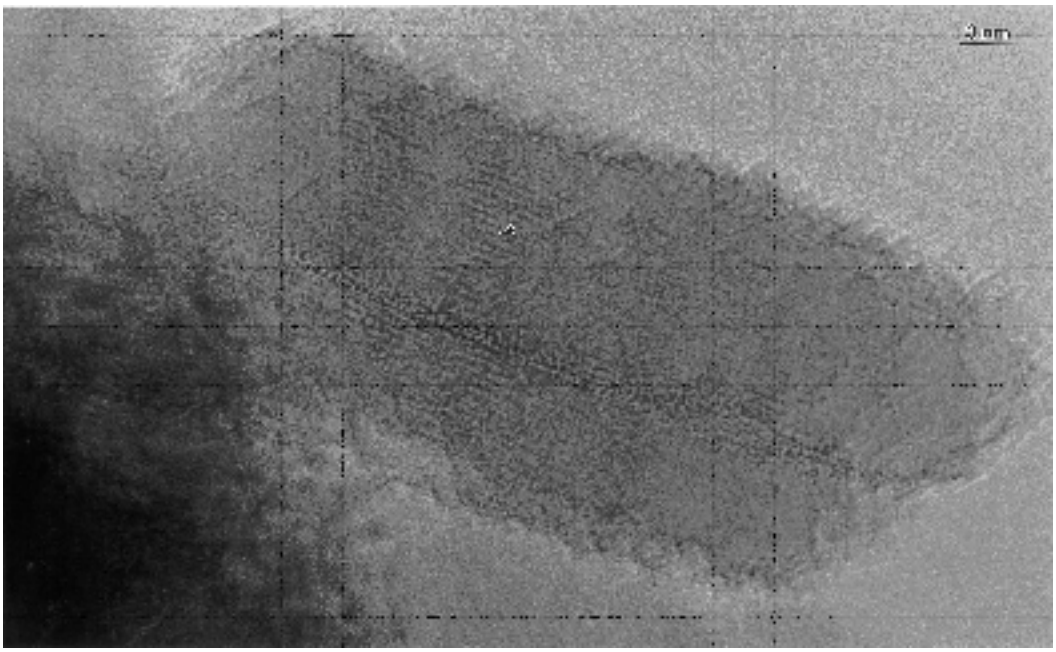

(c)

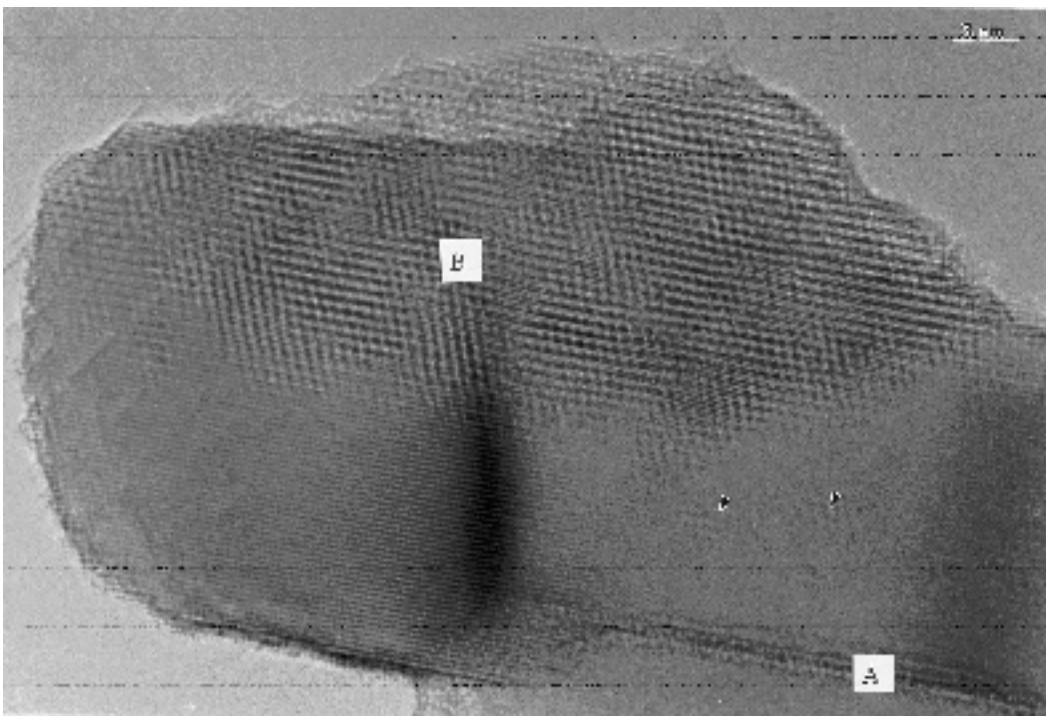

Figure 3. (Continued.)

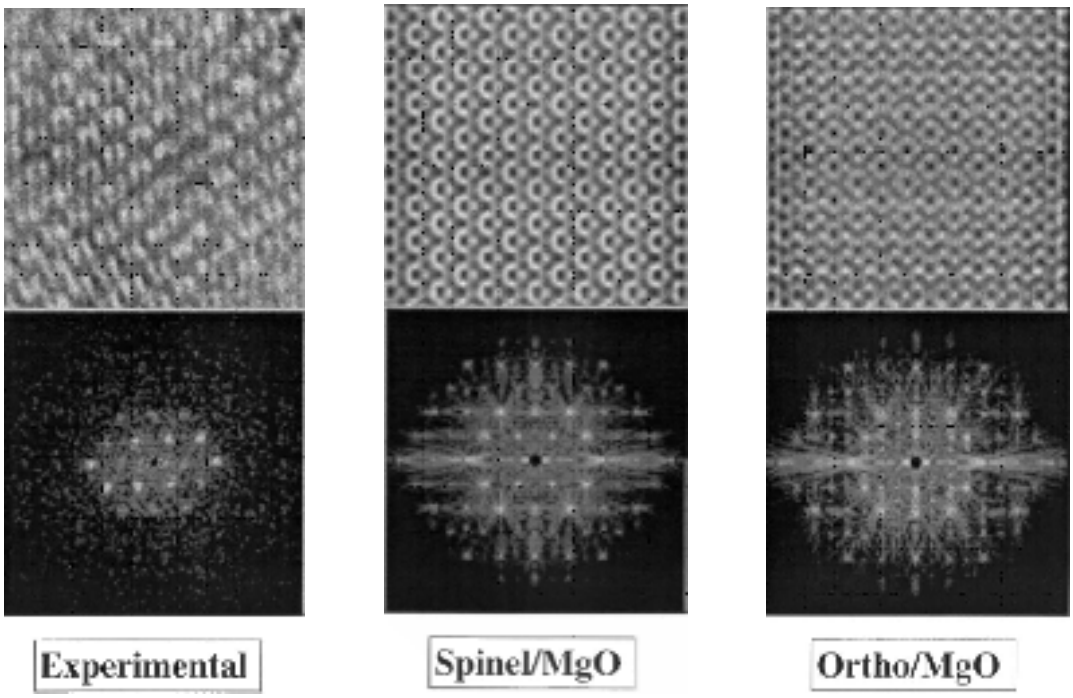

Figure 4. Comparison of an experimental image and associated digital diffraction pattern (DDP) (a) with two simulated models and corresponding DDPs of (b) cubic spinel supported on MgO and (c) orthovanadate supported on MgO (see text for crystallographic details).

the structure of the ordered overlayer, it is either the cubic spinel viewed along the [110] direction or the orthorhombic $Mg_3V_2O_8$ structure viewed along [100]. The former option is the most attractive since the vanadium ions are in the 3+ oxidation state consistent with the EXAFS results. Furthermore, if the spinel is in parallel epitaxy with the MgO support, then the lattice mismatch between the two is only 0.23%. In order to distinguish between the two possible structures, detailed image simulations have been carried out by constructing supercells with the aid of the RHODIUS program [11].

Two supercells have been built using the following epitaxial relationships:

(a) MgO[100]//MgV_2O_4[100] and MgO[011]//MgV_2O_4 [011];

(b) MgO[100]//$Mg_3V_2O_8$[001] and MgO[011]//$Mg_3V_2O_8$ [100].

In case (a), the MgO (011) plane has been matched to the MgV_2O_4 (011) plane. In case (b) MgO (011) has been matched to the $Mg_3V_2O_8$ (100) plane. This ensures that when images are simulated along MgO [011] that the interface plane is normal to the beam direction. When constructing these models we have assumed that the anion sublattice is continuous across the interface. Multislice calculations were carried out assuming an overlayer thickness of 12 Å and a support thickness of 60 Å. Figure 4(a) is a characteristic experimental image of the ordered V-containing layer accompanied by its digital diffraction pattern (DDP). Presented in figure 4 (b) and (c) are the simulated images/DDPs for MgV_2O_4/MgO and $Mg_3V_2O_8$/MgO, respectively. Although neither of the simulated images is a perfect match with the experimental image, they both show fringe periodicities and intersection angles that are consistent with figure 4(a). Hence, on the basis of images alone we cannot state which of the two models is correct. However, if the DDPs are compared it is apparent that the spinel overlayer (figure 4(b)) is a close match to the experimental DDP whereas the orthovanadate overlayer is a poor match; in particular note the presence of the four MgV_2O_4 $\{1\bar{1}1\}$ reflections which are closest to the transmitted beam. A much more in-depth analysis of these structural models, taking into consideration the effects of crystal tilt, interface planes and various layer and substrate thicknesses, will be published elsewhere in the near future [14].

The effects of the different reaction atmospheres on the bulk VMgO material (which constitutes the minor component of the catalyst) are shown in figure 5. Figure 5(a) is a typical HREM micrograph of an $Mg_3V_2O_8$ particle observed in the as-prepared catalyst which, after measurement of the lattice fringe spacings and intersection angles, is oriented along the $[4\bar{3}\bar{2}]$ zone axis. Although the *in situ* XRD experiments suggest a direct conversion of the magnesium orthovanadate to a cubic spinel structure under reaction conditions, TEM observations reveal a more complicated story. Figure 5(b) is an HREM image of a V–Mg–O particle (as determined by EDX) after reaction conditions in which the bulk of the particle is poorly crystalline. This could be an intermediate state between the orthovanadate and the formation of the cubic spinel phase. Indeed, careful inspection

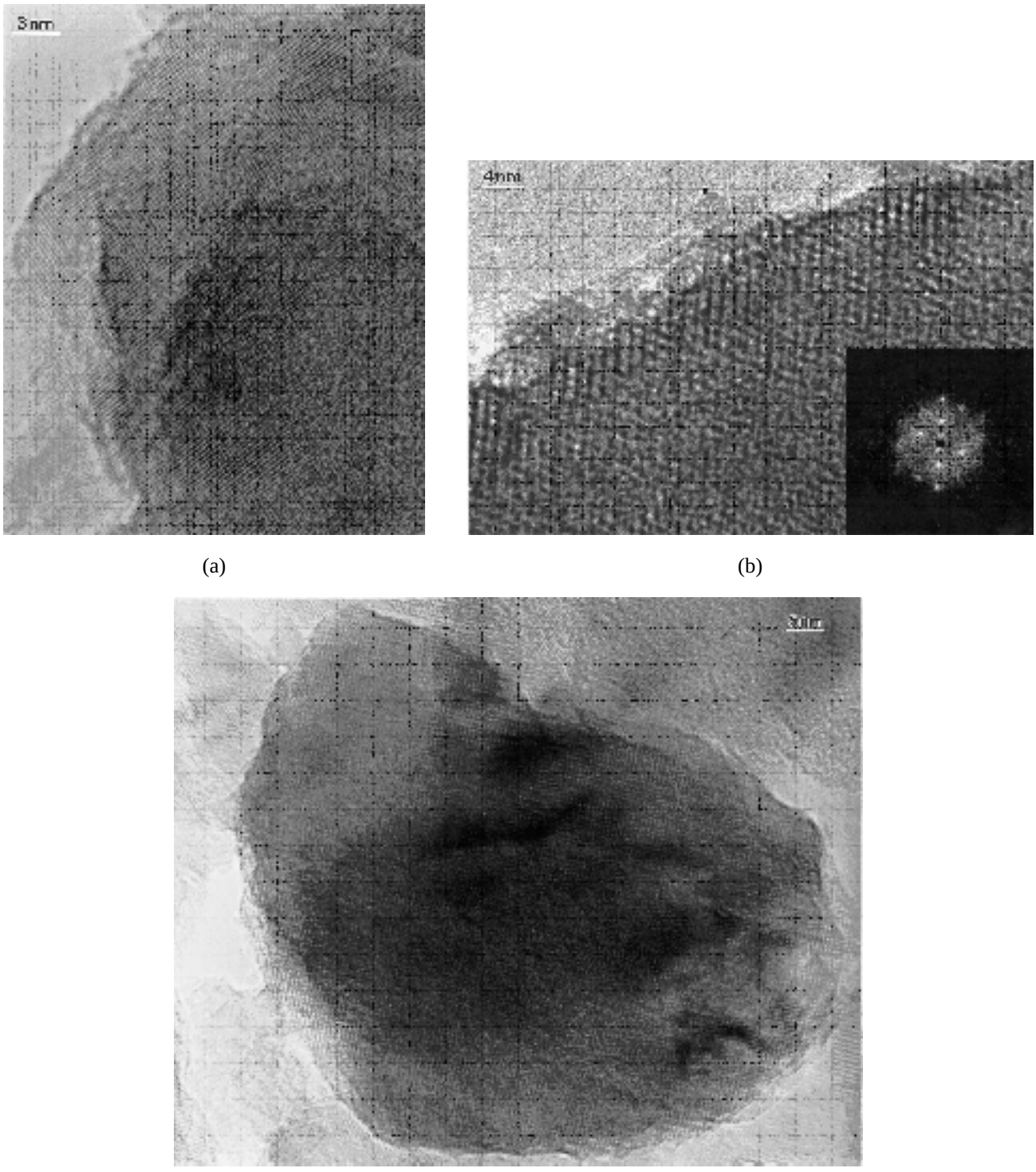

Figure 5. (a) HREM micrograph of an orthovanadate particle observed in the unused catalyst. (b) HREM micrograph and DDP (inset) of a poorly crystalline V–Mg–O particle after exposure to typical ODHP reaction conditions at 500 °C. The arrow indicates a discrete MgO particle. (c) HREM micrograph of a cubic spinel particle observed in the sample exposed to pure propane at 500 °C.

of the periphery of this particle reveals two very relevant features, namely discrete MgO particles at the exterior (arrowed) and just beneath this a thin crystalline spinel layer. DDP analysis of the area indicated superimposed [110] patterns for both MgO and MgV_2O_4 in parallel epitaxy (see inset). The presence of these surface layers in the partially transformed material is most likely a consequence of the following decomposition process:

$$Mg_3V_2O_8 \rightarrow 2MgO + MgV_2O_4 + 2O$$

whereby lattice oxygen becomes available for the Mars–van Krevelen reaction mechanism.

The phase transformation from $Mg_3V_2O_8$ to a bulk crystalline spinel structure under a pure propane atmosphere proved to be more conclusive from the point of view of TEM observations. Figure 5(c) shows a typical HREM micrograph of a VMgO particle which is approximately 80 nm in size. Measurements of the lattice fringe periodicity and intersection angles show them to be consistent with a cubic spinel structure viewed from the $[01\bar{1}]$ direction. After exposure to an atmosphere of air in the reactor at 500 °C these spinel particles remained stable and did not revert back easily to the orthovanadate phase.

4. Discussion

The *in situ* EXAFS and XRD experiments have both indicated that the VMgO catalyst system is structurally sensitive to the reaction atmosphere. A change in the oxidation state of the vanadium from V^{5+} to V^{3+} in the EXAFS spectrum under typical reaction conditions is interpreted in the XRD profile as a phase transformation of magnesium orthovanadate to a cubic spinel structure, MgV_2O_4 (with a lattice parameter of 8.42 Å). Furthermore, this transformation has been found to be reversible on re-exposure to air at typical reaction temperatures, although the XRD pattern demonstrates that the crystallinity of the orthovanadate is of poorer quality compared to the unused material. The reversibility between the V^{5+} and V^{3+} oxidation states during redox cycles correlates well with *in situ* electrical conductivity measurements performed by Pantazidis et al. [10]. Although the existence of a spinel phase in a VMgO catalyst has been proposed by Oganowski et al. [13], no great significance appeared to be attached to its presence; rather it was reported as a precursor in the formation of the $Mg_3V_2O_8$ phase which was considered to be the active surface phase.

Electron microscopy observations support the overall findings of the *in situ* experiments (viz. the presence of MgO and $Mg_3V_2O_8$), but more importantly show details that cannot be inferred from either the XRD pattern or the EXAFS spectrum. In particular, HREM has revealed the presence of a disordered V-containing layer on the MgO which undergoes partial ordering under typical reaction conditions. Understanding the structural nature of this partially ordered layer is crucial, since the vast majority of the vanadium ions available to participate in the catalysis are present in this highly dispersed phase. This was the motivation for reducing the catalyst even further to accelerate the transformation process which serves to transform this layer to a more ordered structure. HREM in conjunction with image simulation and DDP analysis convincingly demonstrates the tendency of the layer to crystallise as MgV_2O_4 in parallel epitaxy with the MgO. Subsequent reoxidation of the catalyst at 500 °C in air does not cause the overlayer to form an epitaxial orthovanadate layer on the MgO, rather it reverts to its initial disordered state.

Electron microscopy has not conclusively shown the presence of a bulk cubic spinel phase after exposure to a typical reaction atmosphere. It would appear these conditions are not severe enough to effect a complete $Mg_3V_2O_8$ to MgV_2O_4 transformation which correlates well with the partial ordering of the overlayer and partially transformed bulk VMgO particles. Hence, the XRD pattern does not revert to that of the "as-prepared" material when the catalyst is exposed to air at 500 °C. It is apparent that under mildly reducing atmospheres the conversion of bulk magnesium orthovanadate to a cubic spinel structure is confined to the first few atomic layers with the interior of these particles in a disordered state. Only when the reaction atmosphere has been changed to pure propane does the complete conversion to a stable bulk spinel phase occur. It is interesting to note that, after subsequent exposure to air at 500 °C for 5 h, the bulk spinel particles remain unchanged, although it is conceivable that a few surface layers have back transformed to the orthovanadate.

Acknowledgement

The authors gratefully acknowledge the technical assistance of Erik Törnqvist (EXAFS), Alfons Maria Molenbroek and Jørgen Villadsen (XRD) and Niels Blom (catalyst preparation). We also thank Dr.'s A. Pantazidis, C. Mirodatos and J.-C. Volta and Mr. J.C. Jalibert for helpful discussions. This work was funded by the EEC under the JOULE programme, contract no. JOE3CT950022.

References

[1] A. Pantazidis, Ph.D. thesis, Université Claude Bernard, Lyon I (1996).
[2] M.A. Chaar, D. Patel and H.H. Kung, J. Catal. 109 (1988) 463.
[3] D. Siew Hew Sam, V. Soenen and J.-C. Volta, J. Catal. 123 (1990) 417.
[4] P.M. Michalakos, M.C. Kung, I. Jahan and H.H. Kung, J. Catal. 140 (1993) 226.
[5] D.L. Stern, J.N. Michaels, L. DeCaul and R.K. Graselli, Appl. Catal. A 153 (1997) 21.
[6] J.N. Michaels, D.L. Stern and R.K. Graselli, Catal. Lett. 42 (1996) 135, 139.
[7] A. Pantazidis, A. Auroux, J.-M. Herrmann and C. Mirodatos, Catal. Today 32 (1996) 81.
[8] A. Pantazidis and C. Mirodatos, Stud. Surf. Sci. Catal. 101 (1996) 1029.
[9] W. Oganowski, J. Hanuza, L. Kępiński, W. Mišta, M. Mączka, A. Wyrostek and Z. Bukowski, J. Mol. Catal. A 136 (1998) 91.
[10] A. Pantazidis, A. Burrows, C.J. Kiely and C. Mirodatos, J. Catal. 177 (1998) 325.
[11] F.J. Botana, J.J. Calvino, G. Blanco, M. Marcos and J.A. Pérez-Omil, Electron Microscopy 2B (1994) 1085.
[12] P. Stadelmann, Ultramicroscopy 21 (1987) 131.
[13] W. Oganowski, J. Hanuza and L. Kępiński, Appl. Catal. A 171 (1998) 145.
[14] J.A. Pérez-Omil, C. López-Cartes, J.J. Calvino, C.J. Kiely and A. Burrows, Ultramicroscopy (1998), in preparation.